

Investigation of 54- to 99-MeV ${}^6\text{Li}$ -induced reactions on rare earth targets

J. G. Fleissner, D. A. Rakel, F. P. Venezia,* E. G. Funk, and J. W. Mihelich
University of Notre Dame, Notre Dame, Indiana 46556

H. A. Smith, Jr.

Indiana University Cyclotron Facility and Physics Department, Indiana University, Bloomington, Indiana 47401

(Received 11 July 1977)

Cross section measurements for the reactions ${}^{150}\text{Sm}$ and ${}^{142,146,150}\text{Nd}({}^6\text{Li}, xn + yp)$ have been performed in the 50–100-MeV energy range. The experimental excitation functions have been compared to the predictions of the geometry dependent hybrid model. Reasonable agreement between theory and experiment is achieved for the (xn) exit channels while significant differences exist for charged particle exit channels. These differences can be attributed to a contribution from breakup of the ${}^6\text{Li}$ projectile with reactions being induced by the breakup fragments.

NUCLEAR REACTIONS ${}^{150}\text{Sm}$, ${}^{142,146,150}\text{Nd}({}^6\text{Li}, xny\beta\gamma)$, enriched targets, E
 = 54–99 MeV; measured in-beam, decay γ rays. Deduced Eu, Sm isotopic
 yields. Geometry-dependent hybrid model; breakup of ${}^6\text{Li}$.

I. INTRODUCTION

With the availability in recent years of a great variety of heavy ion beams and accelerators which can produce energies in the range of tens of MeV per nucleon, it has become feasible to produce nuclei far off the line of stability. An important feature in the study of these nuclei is the excitation function, i.e., cross section measurements as a function of incident projectile energy. These excitation functions, while providing information on the optimum conditions for producing the nuclei of interest, also give information on reaction mechanisms. At present much data are available for protons, deuterons, and α particles with incident energies up to 50 MeV/nucleon; however, little data exist for particles having $A > 4$, especially in the high energy region. Studies have shown that for lithium ions of $E < 10$ MeV/nucleon, breakup of ${}^6\text{Li}$ into its cluster components, an α particle and a deuteron, is an important contribution to the total cross section.^{1,2} Recently Kropp *et al.*³ have carried out excitation function measurements for 48–156-MeV ${}^6\text{Li}$ ions on Au and Ir targets and they conclude from their particle spectra that there are large contributions to the total cross section from reactions induced by cluster components. Calculations using the geometry dependent hybrid model (GDHM),^{4,5} which has been applied successfully for α -induced reactions in this energy region,⁶ have underestimated the yield of the charged particle exit channels for the ${}^6\text{Li}$ -induced reactions on Au and Ir targets. The large observed cross section for the charged particle exit channels has been attributed to the breakup of ${}^6\text{Li}$ with a transfer of one of the breakup

fragments into the target nucleus, forming a compound nucleus in the preequilibrium stage, while the other fragment simply plays the role of a spectator. Excitation function measurements with 50–100-MeV ${}^6\text{Li}$ ions in the Pd region have also given evidence for the importance of breakup through the enhancement of charged particle emission.⁷ We have performed excitation function measurements for 50–100-MeV ${}^6\text{Li}$ ions on rare earth targets and in this paper we present and discuss our results. (A preliminary report of this work was presented earlier.⁸)

II. PROCEDURE

The cross section measurements were obtained using ${}^6\text{Li}$ ions from the Indiana University Cyclotron Facility at incident energies of 54, 66, 77, 84, 91, and 99 MeV. γ rays from product nuclei were detected with Ge(Li) detectors having efficiencies of approximately 10% positioned 90° relative to the beam direction. Charge normalization was achieved by measuring the amount of charge collected in a Faraday cup.⁷ The targets were isotopically enriched metallic foils of ${}^{142,146,150}\text{Nd}$ and ${}^{150}\text{Sm}$ with thicknesses from 1 to 5 mg/cm². Lithium ions of 50–100-MeV incident energy lose less than 1 MeV in traversing such targets. The ${}^{150}\text{Sm}$ target was used for the study of the $(2pxn)$ exit channels since the ${}^{150}\text{Sm}({}^6\text{Li}, 2pxn)$ reactions populate Eu nuclei which have been studied via ${}^6,7\text{Li}$ -induced reactions at lower energies.⁹ $\text{Nd}({}^6\text{Li}, 2pxn)$ reactions populate Pm nuclei for which little information is yet available.

The data obtained were in-beam γ -ray singles, γ rays prompt relative to the beam bursts, and γ rays delayed relative to the beam bursts. (A

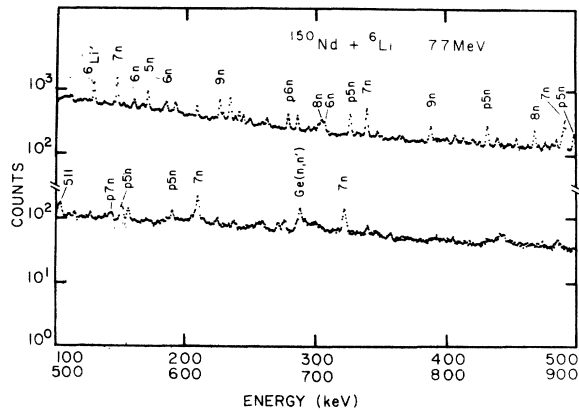


FIG. 1. In-beam γ -ray spectrum from ${}^6\text{Li}$ bombardment of ${}^{150}\text{Nd}$ at 77 MeV. Some of the more intense peaks have been labeled with the appropriate exit channel.

detailed description of the experimental arrangement can be found in Ref. 7.) Residual activities of the targets were also counted off line. Figure 1 shows a typical in-beam singles spectrum with the exit channels labeled for the more intense peaks.

Yields for a particular product nucleus were obtained by summing the intensities of transitions feeding the ground state or a low lying isomeric level. Product nuclei were identified by the presence of at least three known γ -ray transitions and by the relative intensities of these transitions. Table I lists the sources of experimental uncertainties for absolute cross section measurements. A total uncertainty of 20–30% is estimated for an absolute cross-section measurement; however, the relative cross-section measurements at a particular energy are somewhat better.

III. RESULTS AND DISCUSSION

The excitation functions for the (xn) and (pxn) exit channels obtained with the ${}^{150}\text{Nd}$ target are shown in Figs. 2(a) and 2(b) (experimental data are shown as symbols connected by solid lines).

TABLE I. Sources of experimental uncertainties for absolute cross section measurements.

Uncertainty	(%)
Statistical uncertainty	5–20
Absolute γ -ray efficiency	≈ 10
Angular distribution of γ rays	≈ 10
Internal conversion coefficients	< 5
Beam current integration	≈ 10
Dead time effects	< 5
Target thickness	≈ 10
Total uncertainty	20–30

The $(2pxn)$ excitation functions from the ${}^{150}\text{Sm}$ target are shown in Fig. 2(c). Several features are apparent. First, the maximum cross sections for the $({}^6\text{Li}, xn)$, $({}^6\text{Li}, pxn)$, and $({}^6\text{Li}, 2pxn)$ reactions are approximately 300, 200, and 100 mb, respectively. Second, the peak in a particu-

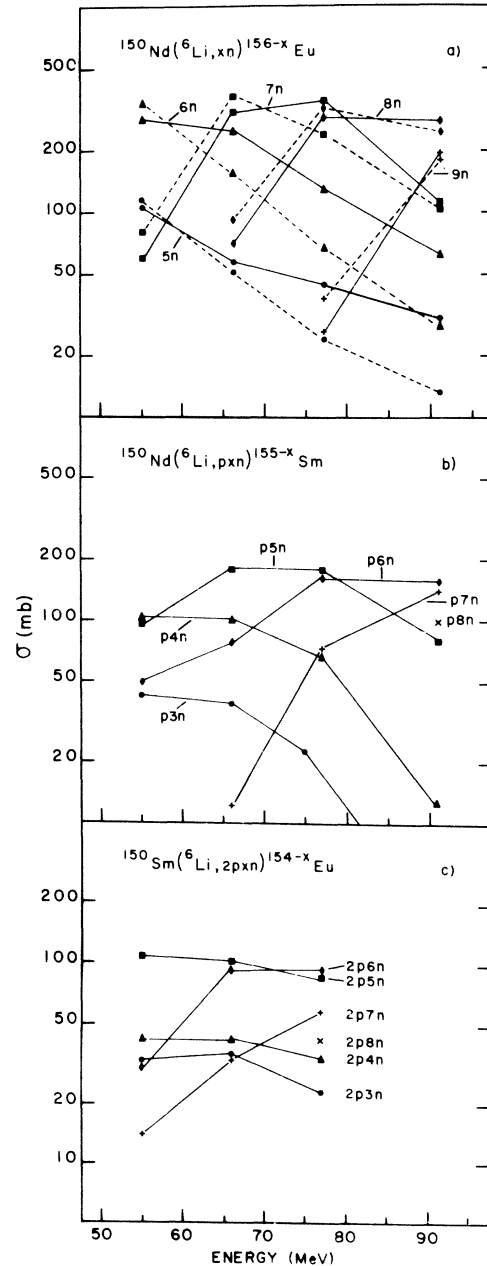


FIG. 2. (a), (b), (c) Energy dependence of the cross section for ${}^6\text{Li}$ on ${}^{150}\text{Nd}$ and ${}^{150}\text{Sm}$. Figure 2(a) is for (xn) exit channels; Fig. 2(b) is for (pxn) exit channels and Fig. 2(c) is for $(2pxn)$ exit channels. Experimental data are shown as symbols connected by solid lines. GDHM predictions are shown as symbols connected by broken lines.

lar (xn) excitation function occurs at approximately 10 MeV per emitted neutron. This agrees with excitation function studies done on rare earth targets in the 26–34-MeV region.⁹ The (pxn) exit channels attain their maximum cross section about 10 MeV higher than the (xn) exit channel with the same number of emitted nucleons, e.g., the cross section for the (${}^6\text{Li}, 7n$) reaction reaches its maximum at about 70 MeV while the maximum for the (${}^6\text{Li}, p6n$) reaction occurs at about 80 MeV. This effect was also noted by Djalois *et al.*⁶ for multi-nucleon emission following α bombardment of ${}^{197}\text{Au}$ targets. Finally, the (pxn) excitation functions seem to have broader maxima and fall off more steeply than the (xn) excitation functions [compare ($5n$) and ($6n$) excitation functions with ($p3n$) and ($p4n$) excitation functions]. The features of the ($2pxn$) excitation functions are not as evident as the (xn) and (pxn) excitation functions obtained from the ${}^{150}\text{Nd}$ target since the ${}^{150}\text{Sm}$ target was irradiated only at 55, 66, and 77 MeV. Nevertheless, the ($2pxn$) excitation functions seem to be characterized by broad maxima similar to the (pxn) exit channels, and to have a gradual decline in cross section as a function of energy similar to the (xn) exit channels.

The data for the lighter mass targets ${}^{142,146}\text{Nd}$, although not as complete as those for the ${}^{150}\text{Sm}$ and ${}^{150}\text{Nd}$ targets due to the lack of information on the level structure for the light Eu nuclei, support the above description of the general features of the excitation functions. Table II lists the experimental cross sections for the four targets used along with the theoretical (GDHM) values for ${}^6\text{Li}$ and breakup fragment-induced reactions. The theoretical values are shown only for those exit channels which were experimentally realizable. Not all targets were run at all energies due to technical difficulties.

The excitation functions obtained in this work are similar to those obtained with ${}^6\text{Li}$ -induced reactions using Au and Ir targets.³ In both of these mass regions, $A \approx 150$ and $A \approx 200$, the (xn) exit channels dominate and the ratios $\sigma(xn)/\sigma(ypxn)$ are approximately the same. In the Pd mass region ($A \approx 100$), however, the charged particle exit channels dominate. The ($ypxn$) cross sections are typically 2 or 3 times larger than the cross sections for the (xn) exit channels. In addition the average number of nucleons emitted as a function of energy⁷ is approximately 0.03 nucleons/MeV for the Pd targets, while for the rare earth targets it is approximately 0.05 nucleons/MeV. For the case of the Pd targets it was suggested⁷ that this small value (0.03 nucleons/MeV as compared with the 0.1 nucleons/MeV value predicted by the fusion-evaporation

model) could be due to the possibility that very little of the additional beam energy is going into the internal excitation of the compound system but is being shared by only a few nucleons. It is perhaps too early to speculate whether the difference between the Pd and rare earth targets is meaningful.

The theoretical predictions of the geometry dependent hybrid model (GDHM) have been compared with the experimentally observed excitation functions. This model describes the nuclear reaction via preequilibrium emission and compound nuclear processes.^{4,5} An adjustable parameter, the number of initial excitons, was fixed at $n_0 = 6$ (three protons and three neutrons) and the nucleon-nucleon mean free path multiplier was taken as unity in all calculations (see Ref. 4).

The broken line in Fig. 2(a) shows the GDHM predictions for the (xn) exit channels. The general shape and positions of the maxima of the excitation functions are reproduced very well but the absolute magnitudes of the theoretical cross sections are 3 times larger than those of the experimental cross sections [theoretical predictions in Fig. 2(a) have been normalized to the experimental results using a χ^2 routine]. This difference in experimental and theoretical absolute cross sections has been noted by Kropp *et al.*³ for ${}^6\text{Li}$ -induced reactions employing Au and Ir targets. One possible explanation for this discrepancy will be discussed below. Others¹ have found it necessary to adjust the mean free path multiplier to fit the GDHM calculations to the experimental results. Another difference is that the high energy tails of the ($5n$) and ($6n$) reactions are predicted to fall off more rapidly than is observed. The main contribution to these high energy tails in the GDHM is from preequilibrium emission and an adjustment of the initial number of excitons would probably correct this deficiency of the theoretical predictions. In their study of α -induced reactions Djalois *et al.*⁶ found an adjustment of the initial number of excitons necessary to describe the high energy tails of the excitation functions, while Jahn *et al.*¹⁰ achieved similar results by varying both the initial number of excitons and the mean free path multiplier.

The shapes of the excitation functions and absolute magnitudes of the cross sections for the (pxn) exit channels are reproduced satisfactorily by the GDHM. Since the theoretical and experimental absolute magnitudes for the (${}^6\text{Li}, pnx$) reactions agree, then it follows that the GDHM predicts a ratio of the maxima of the (xn) and (pxn) cross sections which is 3 times larger than experiment. This "enhancement" relative to the GDHM predictions for charged particle emission will be dis-

TABLE II. Summary of the production cross sections for the $^{142,146,150}\text{Nd}$ and ^{150}Sm targets. The absolute cross sections are quoted in millibarns and with a 25% uncertainty. The $2pxn$ exit channel for the neodymium targets populates promethium nuclei about which little is known; consequently those cross sections are not reported here. The samarium target was used to measure the $2pxn$ cross section: its xn and pxn exit channels populate the less well known terbium and gadolinium nuclei and are not reported here. The top line in the entry for each reaction contains the experimental results. The succeeding lines are the theoretical predictions for the cross sections for the reactions (leading to the same final nucleus) induced by the indicated incident projectile.

Target	Exit channel	Final nucleus	Incident projectile	Energy of ^6Li (MeV)						
				54	66	77	84	91	99	
^{150}Nd	$4n$	^{152}Eu		24		
			^6Li	66	29	17		29		
	$5n$	^{151}Eu		106	57	44		7		
			^6Li	289	132	61		32		
	$6n$	^{150}Eu		284	248	128		61		
			^6Li	1260	575	244		102		
	$7n$	^{149}Eu		59	303	330		110		
			^6Li	203	924	597		258		
	$8n$	^{148}Eu		...	72	303		272		
			^6Li	a	228	805		608		
	$9n$	^{147}Eu		26		185		
			^6Li	b	a	136		652		
	$p3n$	^{152}Sm		42	39	23		3		
			^6Li	38	21	13		5		
			α	60	40	27		17		
			^6Li	96	102	71		13		
	$p4n$	^{151}Sm		71	68	46		21		
			^6Li	659	149	97		68		
	$p5n$	^{150}Sm		96	181	178		80		
			^6Li	25	124	115		63		
$p6n$	^{149}Sm		922	913	287		201			
		^6Li	50	82	174		157			
$p7n$	^{148}Sm		68	68	169		163			
		^6Li	a	695	1210		523			
		α	...	12	73		140			
		^6Li	b	2	86		215			
$p8n$	^{147}Sm		a	a	222		979			
		^6Li		99			
		α	b	a	4		152			
		^6Li	b	b	a		46			
^{150}Sm	$2p3n$	^{151}Eu		32	36	24				
			^6Li	c	c	c				
			d	115	121	119				
			α	4	43	77				
	$2p4n$	^{150}Eu		42	41	34				
			^6Li	c	c	3				
			d	232	220	193				
	$2p5n$	^{149}Eu		a	7	63				
			^6Li	108	102	88				
			d	8	2	2				
	$2p6n$	^{148}Eu		40	179	319				
			^6Li	b	b	2				
			d	31	91	90				
			α	31	21	6				
	$2p7n$	^{147}Eu		b	b	22				
			^6Li	b	b	b				
			d	14	68	58				
			α	c	52	48				
				^6Li	b	b	b			
				α	b	b	b			

TABLE II. (Continued)

Target	Exit channel	Final nucleus	Incident projectile	Energy of ${}^6\text{Li}$ (MeV)						
				54	66	77	84	91	99	
${}^{146}\text{Nd}$	$2p8n$	${}^{146}\text{Eu}$	42					
			${}^6\text{Li}$	a	5	60				
			d	b	b	b				
			α	b	b	b				
	$4n$	${}^{148}\text{Eu}$	
			125	62	28	21	9			
			362	130	21	19	...			
			965	233	132	81	41			
			255	523	181	85	49			
			630	938	353	263	108			
			48	103	179	189	195			
			2	511	942	640	319			
			4	82	211			
			b	c	220	573	532			
			22	39			
			b	b	c	32	424			
			$p3n$	${}^{148}\text{Sm}$	${}^6\text{Li}$	84
					α	51	36	18	11	6
$p4n$	${}^{147}\text{Sm}$	${}^6\text{Li}$	66	52	36	29	16			
		α	124	158	62			
$p5n$	${}^{146}\text{Sm}$	${}^6\text{Li}$	99	119	88	61	31			
		α	1440	290	167	138	89			
$p6n$	${}^{145}\text{Sm}$	${}^6\text{Li}$	52	130	86	79	108			
		α	10	166	193	157	90			
$p7n$	${}^{144}\text{Sm}$	${}^6\text{Li}$	97	1380	813	455	207			
		α	44	97	173			
$p8n$	${}^{143}\text{Sm}$	${}^6\text{Li}$	a	19	185	253	201			
		α	b	30	768	1110	572			
$p9n$	${}^{142}\text{Sm}$	${}^6\text{Li}$	14	32	201			
		α	b	a	27	136	337			
$p10n$	${}^{141}\text{Sm}$	${}^6\text{Li}$	b	b	c	46	814			
		α	63			
$p11n$	${}^{140}\text{Sm}$	${}^6\text{Li}$	b	b	a	5	183			
		α	b	b	b	b	11			
${}^{142}\text{Nd}$	$4n$	${}^{144}\text{Eu}$	384	101		40	...			
			327	116		34	16			
			238	370		106	46			
	$5n$	${}^{143}\text{Eu}$	1150	537		148	59			
				104	...			
			24	770		349	172			
	$6n$	${}^{142}\text{Eu}$			
					
			b	9		540	318			
	$7n$	${}^{141}\text{Eu}$			
					
			b	b		47	282			
	$8n$	${}^{140}\text{Eu}$			
					
			b	b		b	16			
	$p3n$	${}^{144}\text{Sm}$	${}^6\text{Li}$	166	85		24	34		
			α	114	63		25	12		
			α	190	66		38	27		
$p4n$	${}^{143}\text{Sm}$	${}^6\text{Li}$	109	230		143	37			
		α	139	256		127	56			
		α	1360	1150		189	115			
$p5n$	${}^{142}\text{Sm}$	${}^6\text{Li}$	18	61		205	233			
		α	2	176		307	169			
		α	b	452		946	298			
$p6n$	${}^{141}\text{Sm}$	${}^6\text{Li}$		36	126			
		α	b	4		352	363			
		α	b	b		463	968			

TABLE II. (Continued)

Target	Exit channel	Final nucleus	Incident projectile	Energy of ${}^6\text{Li}$ (MeV)					
				54	66	77	84	91	99
	$p7n$	${}^{140}\text{Sm}$	${}^6\text{Li}$		14		59
			α	b	b		65		439
			α	b	b		a		106
	$p8n$	${}^{139}\text{Sm}$	${}^6\text{Li}$
			${}^6\text{Li}$	b	b		a		80
			α	b	b		b		b

^a $10^{-3} \text{ mb} \leq \sigma < 10^{-1} \text{ mb}$.

^b $0 \text{ mb} \leq \sigma < 10^{-3} \text{ mb}$.

^c $10^{-1} \text{ mb} \leq \sigma < 1 \text{ mb}$.

cussed below. The theoretical absolute magnitudes of the cross sections for the $(2pxn)$ exit channels are on the average too small by a factor of about 50 and in some extreme cases by as much as 200. Furthermore, the predictions for the thresholds of certain reactions deviate considerably from those determined experimentally and the shapes of the excitation functions are not reproduced very well.

The enhancement of charged particle emission was not observed in the study of α -induced reactions by Djaloeis but has been observed in d - and ${}^3\text{He}$ -induced reactions¹¹ and ${}^6\text{Li}$ -induced reactions (in both the Pd (Ref. 7) and Au-Ir mass regions³) and has been attributed to breakup of the incident projectile. Particle spectra obtained by Kropp *et al.*³ for ${}^6\text{Li}$ incident on Au and Ir targets show groups of α particles and deuterons with velocities distributed about the original beam velocity indicating the importance of the cluster structure for ${}^6\text{Li}$. They estimate a differential cross section of approximately 1.5 b/sr at $\theta_{\text{lab}} = 15^\circ$ for reactions with at least an α particle in the exit channel. They also found considerably more α particles than deuterons suggesting a three particle (${}^6\text{Li} \rightarrow \alpha + p + n$) breakup contribution to the entrance channel. Preliminary results for particle spectra in the Pd mass region are similar to these findings.⁷

Figure 3(a) shows the experimental isotopic yields along with the GDHM predictions for the ${}^{150}\text{Nd}$ and ${}^{150}\text{Sm}$ targets at 66 MeV. In general the Eu yields from the (xn) exit channels agree very well with the GDHM predictions for ${}^6\text{Li}$ -induced reactions. The Sm yields from the (pxn) exit channels are consistent with the "enhancement" for charged particle emission and a typical case is shown in Fig. 3(b). Also shown in Fig. 3(b) are the GDHM predictions of the isotopic yields for the reactions in which the α breakup fragment is taken to be the incident projectile at $\frac{2}{3}$ of the ${}^6\text{Li}$ energy. [In Figs. 3(b) and 3(c) predictions of isotopic yields for ${}^6\text{Li}$ -induced reactions have

been normalized to the $({}^6\text{Li}, xn)$ yields while no normalization was performed for yields corresponding to reactions induced by breakup fragments.] Note that these predictions for fragment-induced reactions reproduce the position of the maximum of the isotopic yield curve correctly. There are significant discrepancies between theory and experiment for the Eu yields from the $(2pxn)$ exit channels, and a typical case is shown in Fig. 3(c). The GDHM model predictions for ${}^6\text{Li}$ -induced reactions do not reproduce the threshold, position of the maximum, or shape of the isotopic yield curve. The theoretical predictions for the yields induced by α and d breakup fragments at $\frac{2}{3}$ and $\frac{1}{3}$ the beam energy, respectively, agree more closely with experiment although the maximum in the yield curve differs by 1 mass unit. The agreement could be improved by inclusion of three particle breakup since the $(p, 2n)$ reaction would be energetically possible. In addition, since the cluster fragments have distributions in velocities about the beam velocity, a consideration of this would change the shape of the theoretical isotopic

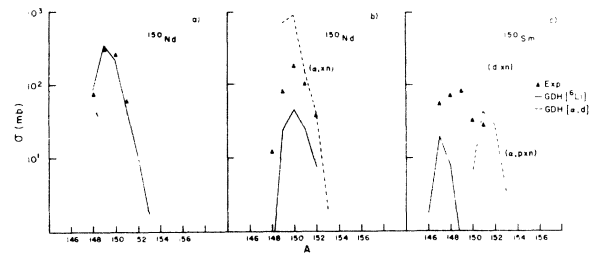


FIG. 3. (a), (b), (c) Experimental and theoretical yields of 66-MeV ${}^6\text{Li}$ -induced reactions as a function of A of the product nucleus. Figure 3(a) is for (xn) exit channels; Fig. 3(b) is for (pxn) exit channels and Fig. 3(c) depicts $(2pxn)$ exit channels. Experimental data are shown as symbols. GDHM predictions for ${}^6\text{Li}$ -induced reactions are shown as solid lines, while predictions for breakup fragment induced reactions are shown as dashed lines. See text for a discussion of normalization procedure.

yield curve. The discrepancy in absolute magnitude noted above for the (αn) reactions could then be attributed to the loss of ${}^6\text{Li}$ incident flux due to breakup reactions.

It is interesting to note that the GDHM predicts for ${}^6\text{Li}$ fusion a significant increase in the charged particle exit channel yields for the more neutron deficient ${}^{142}\text{Nd}$ as compared with ${}^{150}\text{Nd}$. The fact that this increase is not observed experimentally may be due to the importance of the breakup of ${}^6\text{Li}$ in the production of charged particle exit channels.

IV. CONCLUSION

The results obtained in this work extend the experimental information in the rare earth region for ${}^6\text{Li}$ -induced multinucleon emission reactions to considerably higher energies. The geometry dependent hybrid model which has been applied successfully to α -induced reactions has shown

certain deficiencies when its predictions are compared with the experimental results for ${}^6\text{Li}$ -induced reactions. These deficiencies may be attributed to the cluster structure of the ${}^6\text{Li}$ projectile. Better agreement between theory and experiment is achieved when breakup fragments are included in the entrance channel.

ACKNOWLEDGMENTS

The authors would like to thank Mr. S. Rozak and Dr. T. Ward for their assistance in data collection and Professor Darwin J. Mead for his help in preparing the figures. The technical support of the Indiana University Cyclotron Facility operating crews is gratefully acknowledged. We also extend our thanks to Professor Marshall Blann for providing both a copy of his computer code for the GDHM calculations and some helpful discussions. Work supported by the National Science Foundation.

*Present address: Bellarmine College, Louisville, Kentucky 40205.

¹R. Ollerhead, C. Chasman, and D. Bromley, *Phys. Rev.* **134**, B74 (1964).

²K. Bethge and K. Meier-Ewert, *Phys. Rev. Lett.* **18**, 1010 (1967).

³J. Kropp *et al.*, *Z. Phys.* **A280**, 61 (1977).

⁴M. Blann, *Annu. Rev. Nucl. Sci.* **25**, 123 (1975).

⁵M. Blann, University of Rochester Report No. COO-3494-29, 1976 (unpublished).

⁶A. Djalois, P. Jahn, H-J. Probst, and C. Mayer-Böricke, *Nucl. Phys.* **A250**, 149 (1975).

⁷C. Castaneda, H. A. Smith, T. Ward, and T. Nees, *Phys. Rev. C* **16**, 1437 (1977).

⁸J. Fleissner *et al.*, *Bull. Am. Phys. Soc.* **21**, 1006 (1976).

⁹J. Fleissner, E. Funk, F. Venezia, and J. Mihelich, *Phys. Rev. C* **16**, 227 (1977).

¹⁰P. Jahn *et al.*, *Nucl. Phys.* **A209**, 333 (1973).

¹¹A. Chevarier *et al.*, *Nucl. Phys.* **A237**, 354 (1975).